On the Design, Development and Motion Control of a Humanoid Robotic Leg via Pneumatic Artificial Muscles

George Andrikopoulos, *Member, IEEE*, George Nikolakopoulos, *Member, IEEE*

***Abstract*— In this article, the design and implementation of a HUmanoid Robotic Leg (HURL) is presented. The motion of the HURL is achieved via pneumatic muscle actuators, a pneumatic form of actuation possessing crucial attributes for the implementation of a biomimetic design that mimics the motion characteristics of a human ankle. The HURL's properties are described in detail, while its 2-DoF motion capabilities (dorsiflexion - plantar flexion, eversion - inversion) are experimentally evaluated via an advanced nonlinear PID-based control algorithm.**

I. Introduction

In this article, the conceptual design of a novel HUmanoid Robotic Leg (HURL) is presented, which possesses the mechanical ability of reproducing the 2 Degree of Freedom (DoF) movement capabilities of the human ankle: a) dorsiflexion/plantar flexion, and b) inversion/eversion [1]. Such a robotic appliance is considered as the initial conceptual point and mandatory infrastructure for enabling future interactive applications on lower-limb balance research driven by smooth, fast and accurate movements, while its experimental evaluation acts as the feasibility study for the future development of a balancing humanoid robot.

For actuation purposes, the HURL utilizes Pneumatic Muscle Actuators (PMAs) in order to achieve 2-DoF movements performed via its ankle-inspired joint. The PMA is a tube–like pneumatic actuator that is characterized by a decrease in the actuating length when pressurized, while possessing similar properties with those of the organic muscle, combined with several advantages as the ability to provide high power outputs, with relatively light weights and inherent compliance [2]. These characteristics are turning the PMA into a promising actuator choice in anthropomatic technologies, while a variety of such applications have already been appeared in the literature [3]. Moreover, PMA meets the need for safety, simplicity and lightness that human–robot interaction requires and justifies its expanding utilization in medical and biorobotic applications.

The main contribution of this article stems from the design of a humanoid leg via the utilization of PMA technology, as well as the feasibility study performed through the development and experimental evaluation of a PMA-actuated pneumatic leg. It has to be noted that the proposed PMA configured design is proposed and experimentally evaluated for providing an alternative mechanical solution to similar approaches identified in related literature [4]–[11]. The proposed design is evaluated as a basic motion problem, however, the conceptual design from an engineering point of view and without losing generalization, can form the basis for its expansion in developing a compliant, safe and motion accurate lower-limb humanoid, while possessing the necessary biomimetic attributes for its alternative use as a prosthetic leg appliance.

The rest of the article is structured as follows. In Section II, the design specifics of the HURL as well as its motion capabilities are presented in detail. Section III presents the synthesized control algorithm for the undertaking of the HURL's motion. Section IV provides an overview of the various components utilized in the implementation of the HURL prototype, while in Section V, open and closed loop experimental results for the evaluation of the HURL's 2-DoF motion capabilities are presented, with the closed loop evaluation performed via the utilization of an advanced non-linear PID-based control algorithm. Finally, the conclusions are drawn in Section VI.

II. Conceptual Design of the HURL

A. Design Specifics

The number and placement of the PMAs for the actuation of the HURL appliance was properly chosen in order to simplify the complexity of the ankle movement scenarios (dorsiflexion/plantar flexion and inversion/eversion). As shown in Fig. 1, the proposed design utilizes two antagonistic PMA pairs placed in cross-formation around the Tibia/Fibula-inspired bone and with the intersecting plane of each pair being parallel to the target plane of motion.

This design aspect provides the significant advantage of mechanically decoupling the HURL's 2 DoFs, as each pair of PMAs is structurally responsible for the generation of one respective movement. This design aspect differs from the synergy-based human muscle operation, where muscle groups are involved in the generation of more than one movements of the human foot [12]. As presented in the next Subsection, this biomimetic simplification led to a motion strategy defined by one manipulated variable per PMA pair, thus also simplifying the motion control problem.

The motion transfer mechanism utilizes tendon wires that connect the PMAs via caps to the HURL's heel-inspired formation via appropriately placed connection points (Fig. 1(c)). The caps involve a choke mechanism for the placement and easy adjustment of the tendon wires during operation, while four linear motion shafts are incorporated in the Tibia/Fibula bone design for the connection with the PMA caps, which operate as prismatic joints in order to enforce the linear motion of the PMAs and compensate for any non-axial forces exerted during complex motion scenarios (Fig. 1(b)).

*Research supported by the Swedish Research Council (Vetenskapsrådet).

G. Andrikopoulos and G. Nikolakopoulos are with the Control Engineering Group, Luleå University of Technology, SE-97189 Luleå, Sweden, E-mail: {geoand, geonik} @ltu.se

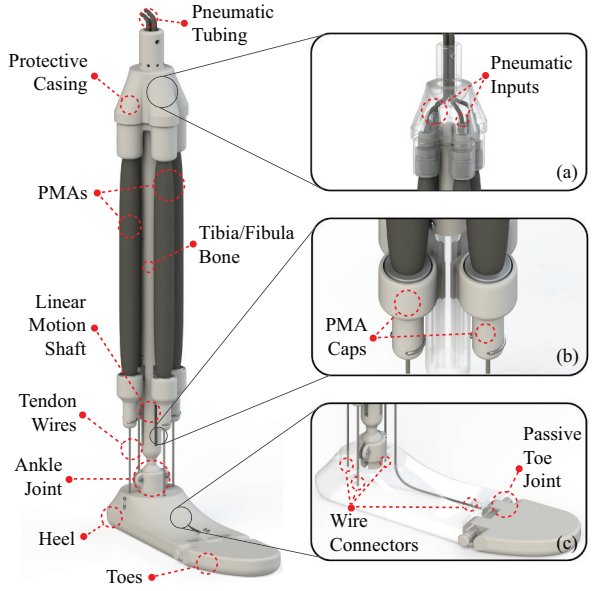

Fig. 1. Overview of the HURL design specifics.

It has to be noted that the wire connection points on the heel are distributed along the spherical joint that plays the role of a simplified ankle-inspired mechanism, but the front tendon wire that is responsible for the flexion movements is driven through the foot's bridge area, and finally gets attached to the connection point resembling the mound of a toe-inspired formation (Fig. 1). This particular strategy was identified as most suitable for the better distribution of forces during operation, which is crucial due to the asymmetry of the foot along its longitudinal axis, while mimicking the placement of the extensor tendons in the human foot [12], i.e. the main tendons responsible for the dorsiflexion and inversion movements. Finally, the toe-inspired formation is connected to the main foot section via a passive joint, which incorporates a torsion spring in order to restrict unwanted toe movements during the HURL's operation.

B. Motion Strategy

The selected movement strategy for the replication of the ankle's 2-DoF motion capabilities is graphically represented in Fig. 2. Green color highlights the PMAs in idle (initial) contracted state, blue color highlights the inflated PMAs, while the deflated PMAs are highlighted with red color.

Specifically, in order to take advantage of the full PMA stroke and thus, ensure the maximum provided range of motion for every DoF, the PMAs are initially inflated at a P_0 pressure which corresponds to the half of their maximum permissible stroke, before being connected to their respective tendons. With that in mind, the utilized antagonistic movement strategy is formulated as:

$$P_{i,j} = P_{i,0} \pm \Delta P_i \tag{1}$$

$$\text{for} \begin{cases} i=1 \text{ and } j=1,2 \text{ with} \begin{cases} \Delta P_1 > 0 \Rightarrow \text{Dorsiflexion (Fig. 4(b))} \\ \Delta P_1 < 0 \Rightarrow \text{Plantar Flexion (Fig. 4(c))} \end{cases} \\ i=2 \text{ and } j=1,2 \text{ with} \begin{cases} \Delta P_2 > 0 \Rightarrow \text{ Eversion (Fig. 4(d))} \\ \Delta P_2 < 0 \Rightarrow \text{ Inversion (Fig. 4(e))} \end{cases} \end{cases},$$

where $P_{i,j}$ defines the pressure values utilized in every antagonistic pair of PMAs and identified as j=1,2, for the undertaking of the i = 1,2 DoF movements of dorsiflexion/plantar flexion and inversion/eversion respectively, while $P_{i,0}$ denotes the initial pressure of the i-th PMA pair. This strategy has the advantage of utilizing one manipulated pressure variable ΔP_i per antagonistic PMA pair and depending on its sign leads to the activation of the target motion pattern.

III. Motion Control

In the concept of evaluation of the HURL's operation, the ANPID algorithm, due to its increased flexibility and adaptability, as well as its experimentally verified capability in producing smooth, fast and accurate PMA responses [13], has been considered as a suitable choice for undertaking the motion control problem of the ankle exoskeleton. The purpose of the ANPID-based control scheme is to provide a preliminary evaluation of the HURL's performance. The development and evaluation of more complex control structures for torque and compliance control is part of future work.

The movement strategy described in (1) significantly simplifies the motion control problem, since every scenario involves only one control variable, the manipulated pressure ΔP_i, which is transferred via the same strategy to the PMAs of the HURL. For this reason, the HURL's motion control problem will be addressed via the use of a double ANPID-based control structure under the assumption of a sampling process with a sampling period $T_s \in \mathbb{R}^+$, while at sample $n \in \mathbb{Z}^+$.

The ANPID algorithm, while compared to the standard PID structure [14], features additional tuning modes for its basic control parameters, i.e. the proportional gain K_P, the reset time T_I in minutes and the rate time T_D in minutes, which synthesize the following modified error signals e_P, e_I and e_D for the proportional, integral and derivative control action terms, respectively:

$$\begin{aligned} e_P(n) &= \frac{\left[f x_{\text{ref}}(n) - x(n)\right]}{x_{\text{ref,range}}}\left[g x_{\text{ref,range}} + (1-g)\left|f x_{\text{ref}}(n) - x(n)\right|\right], \\ e_I(n) &= \frac{\left[x_{\text{ref}}(n) - x(n)\right]}{x_{\text{ref,range}}}\left[g x_{\text{ref,range}} + (1-g)\left|x_{\text{ref}}(n) - x(n)\right|\right], \\ e_D(n) &= \frac{\left[q x_{\text{ref}}(n) - x(n)\right]}{x_{\text{ref,range}}}\left[g x_{\text{ref,range}} + (1-g)\left|q x_{\text{ref}}(n) - x(n)\right|\right]. \end{aligned} \tag{2}$$

where $x_{\text{ref,range}}$ denotes the range of the reference output x. The mode selector $f \in [0,1]$ is utilized as a relative trade-off between noise rejection and set-point tracking; f=1 results in error-affected action and control emphasis on tracking the reference signal, while f=0 results in measurement-affected action and emphasis on disturbance cancellation. The mode selector $q \in [0,1]$ accounts for differentiation on error (q=1) or measurement (q=0). When q is posed on measurement, it reduces the derivative kick effect and results in reverse-acting control operation [14].

Furthermore, in order to achieve an adjustable decrease of K_p gain at low error magnitudes and the corresponding gradual increase at large deviations from the set-point, the linearity factor $g \in [0,1]$, is properly introduced in (2) to

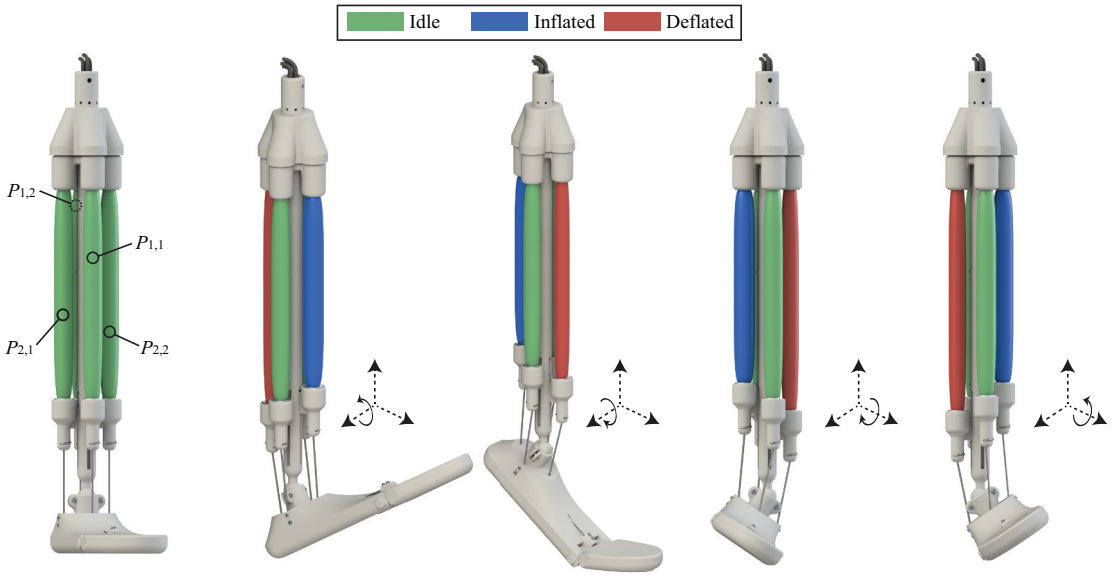

Fig. 2. Graphical representation of the HURL movement strategy during: (a) Idle, (b) Dorsiflexion, (c) Plantar Flexion, (d) Eversion, and (e) Inversion.

account for the increase in K_p, with respect to the error's magnitude. In this manner, the ANPID achieves further customization of control behavior at different error magnitudes via an auto-adjustable gain.

Finally, the discrete time control action $u(n)$ of the ANPID algorithm is being formulated as shown below:

$$u(n) = K_P\left[e_P(n) + \delta\frac{T_s}{T_I}\sum_{i=1}^{n}\left[\frac{e_I(i)+e_I(i-1)}{2}\right]h(i) + \frac{T_D}{T_s}\left[e_D(n)-e_D(n-1)\right]\right]. \quad (3)$$

where $h(n) = \left(\frac{x^2_{\text{ref,range}}}{x^2_{\text{ref,range}} + 10e_I^2(n)}\right)$ defines the discrete representation utilized for the nonlinear adjustment of the internal term in order to counteract overshoot phenomena. In addition, a switch function δ that is defined in (4):

$$\delta = \begin{cases} 1 & \text{for } u_{\min} \le u(n) \le u_{\max} \\ 0 & \text{if } u(n) \le u_{\min} \text{ or } u(n) \ge u_{\max} \end{cases}, \quad (4)$$

is incorporated in the integral control action of (3) to avoid the intense overshoot phenomena that follow cases of a constant error factor, due to e.g. a proportional pressure regulator reaching its output limits, where the integral action drives the control effort to its extreme values $u_{\min}$ or $u_{\max}$, resulting in a saturated condition called "wind-up". In this case, two ANPID algorithms are utilized for the control of the two angular motions. Specifically, in each ANPID the manipulated variable u responds to the pressure ΔP_i presented in (1), the mode selectors are properly defined as f_i, q_i, and g_i. The process value x is the angular motion θ_i that leads to the following error definition:

$$e_i = \theta_{i,\text{ref}} - \theta_i \quad (5)$$

or equivalently denoting the dorsiflexion/plantar flexion and inversion/eversion movement types, defined by θ_1 (°) and θ_2 (°) respectively, while $\theta_{1,\text{ref}}$ and $\theta_{2,\text{ref}}$ are their respective reference angle values. The selected orientation for both process angle values is kinetically translated as:

$$\theta_1 \begin{cases} > 0 \Rightarrow \text{Dorsiflexion} \\ < 0 \Rightarrow \text{Plantar Flexion} \end{cases} \text{ and } \theta_2 \begin{cases} > 0 \Rightarrow \text{Eversion} \\ < 0 \Rightarrow \text{Inversion} \end{cases}. \quad (6)$$

The utilization of PMAs introduces intense non-linearities, which increase the difficulty in fine-tuning the control parameters K_P, T_I and T_D for achieving efficient control performance throughout the HURL's operating range. For this reason, a gain scheduler is appropriately incorporated in the PID control structure, which has the ability to alter the control parameters K_P, T_I and T_D according to the movement type denoted by the switching signal i and according to the active region of operation, specified by the selected manipulated value. In this case, an additional switching signal $m \in \mathbb{Z}^+$ is introduced that rules the switching values of the previously constant gains, as in the sequel:

$$\begin{bmatrix} K_P^i \\ T_I^i \\ T_D^i \end{bmatrix} = \begin{bmatrix} K_{P,m}^i \\ T_{\text{I},m}^i \\ T_{\text{D},m}^i \end{bmatrix} \text{ for } m=1,2,\ ...,M, \quad (7)$$

where $M \in \mathbb{Z}^+$ is the maximum number of operating regions. In the utilized notation the sub-indexes i and m were utilized as the switching natures of the corresponding variables.

To ensure smooth transition between the areas of operation defined by the aforementioned gain scheduling mechanism, a bump-less mechanism is being utilized, which acts as an integral sum adjustment function by keeping the addition of the proportional and integral actions invariant to parameter alterations. Therefore, during switches between neighboring areas of operation the control effort becomes:

$$\Delta P_i(n) = K_P^i(n-1)e_P^i(n-1) + K_P^i(n)\left[\begin{matrix} \delta\frac{T_s}{T_I^i}\sum_{i=1}^{n-1}\left[\frac{e_I^i(i)+e_I^i(i-1)}{2}\right]h(i-1) + \\ \frac{T_D^i}{T_s}\left[e_D^i(n)-e_D^i(n-1)\right] \end{matrix}\right] \quad (8)$$

Based on the system's characteristics and the desirable control attributes, constraints are posed on the controllers'

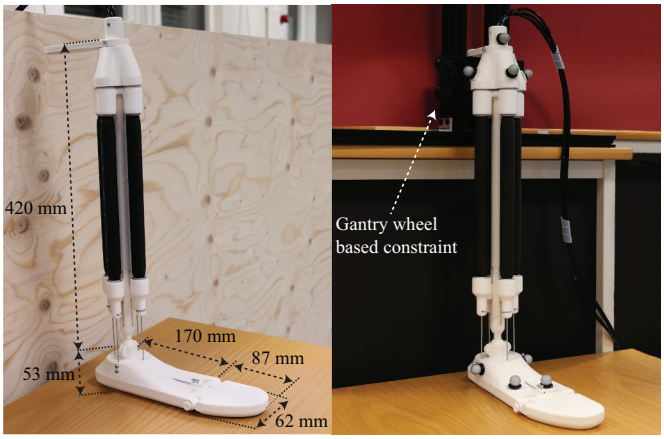

(a) (b)

Fig. 3. The HURL prototype's (a) dimensions, (b) evaluation setup.

outputs $Pi,j(n)$ and set-point values $\theta i,_{\text{ref}}(n)$, by setting minimum and maximum limits as specified in (9):

$$\begin{bmatrix} P_{i,j}^{\min} \\ \theta_{i,\text{ref}}^{\min} \end{bmatrix} \leq \begin{bmatrix} P_{i,\text{j}} \\ \theta_{i,ref} \end{bmatrix} \leq \begin{bmatrix} P_{i,j}^{\max} \\ \theta_{i,\text{ref}}^{\max} \end{bmatrix}. \quad (9)$$

IV. Prototype Development and Setup Components

A. Development of the HURL Prototype

For performing a feasibility study on the proposed robotic appliance, the 2-DoF humanoid leg was developed by following the mechanical strategies described in Section II. The prototype version of the HURL is presented in Fig. 3(a), along with highlights of the basic dimensions of its skeletal structure, which follow a biomimetic approach via replication of the mean dimensions of an adult male's leg [15]. In addition, Fig. 3(b) presents the utilized evaluation setup, which had the HURL's knee formation constrained via the use of a gantry wheel-based system so as to allow only its translational movement along the vertical z axis. The purpose of this particular setup was to evaluate the motions of the HURL's ankle while being under load and mechanically forced to replicate the presented motion patterns. It has to be noted that the wheel-based setup is passive in nature and does not provide any motion support on the HURL.

Overall, four Festo DMSP-10-260N-AM-CM Fluidic Muscles with 10 mm internal nominal diameter and 260 mm nominal length were utilized for the replication of the ankle movements. The nominal length of the PMAs was appropriately selected by taking into consideration the dimension restrictions of the biomimetic design, while the PMAs' placement upon the skeletal structure of the HURL plays a crucial role to the robot's motion quality, since it acts as a trade-off between the acquired angular motion and the torque generated on the ankle joint, considering the fact that the utilized PMAs can be operated between their permissible pressure range 0 to 8 bar.

In addition, low-weight materials were utilized in the development of the skeletal structure in order to minimize the inertial effects of the HURL's equipment during joint motion. As shown in Fig. 3, the skeleton, the various connection components and the joint parts have being 3D printed via PLA material. Also, steel wire was selected for the role of the artificial tendons, while being equipped with plastic coating to decrease the friction phenomena during contact with the 3D-printed joints. This selection of materials led to a robotic leg that weighs approximately 1 kg, of which 0.36 kg belong to the utilized PMAs.

B. Setup Components

Regarding additional setup components, four Festo VPPM-6F-L-1-F-0L10H-V1N-S1 proportional pressure regulators were utilized to control and measure the pressure of the compressed air supplied into the PMAs. The utilized pressure sensors, which are integrated inside the aforementioned pressure regulators, provide a measurement accuracy of ±0.0035 bar. Moreover, a VICON motion capturing system consisted of twenty IR cameras were utilized for the measurement and acquisition of angular and translational motion data of the humanoid leg prototype. The specific equipment ensures high-accuracy measurements, as it provides translation accuracy of approximately 0.04 mm and a respective angular accuracy of 0.02 degrees. Finally, the control of the setup's operation, as well as the data acquisition, were achieved via a USB-1608G and a USB-3100 supplied by Measurement Computing, while the setup's programming software was developed in National Instruments LabVIEW.

V. Experimental Results

Extensive experimental studies were performed to test the HURL's 2-DoFs, as well as to evaluate its performance in reproducing human-like movements through its biomimetic ankle. This Section presents the experimentally acquired results, which include open-loop responses for the evaluation of the HURL's structural capabilities in replicating the human ankle's movements, as well as closed-loop control performances via the proposed ANPID-based structure.

It has to be noted that for all the experimental trials described in the sequel, a sampling period of $T_s = 0.1$ sec was selected, acting as a trade-off between data representation accuracy and overall execution speed based on the utilized computer unit. Moreover, the initial pressures utilized for the joint's idle state were properly tuned as $P_{i,0} = 4$ bar, while all pressure signals, which were calculated via (1) and the appropriate change of the pressure element $\Delta P_{i,j}$, were constrained to the PMA's permissible range $0 \leq P_{i,j} \leq 8$ bar for $i = 1,2$ and $j = 1,2$.

Initially, extensive experimental trials concerning open-loop responses were performed in order to test all possible movement patterns of the HURL. Fig. 4 presents photographs of the setup during different operational states, which were taken throughout these experimental sequences. The angular data of the humanoid ankle were recorded via the VICON motion capturing system, thus providing a highly accurate measurement of the maximum angular range of the HURL's joint with respect to the idle state depicted in Fig. 4(a) and given the maximum pressure range provided via (1). These maximum motion ranges are presented in Table I in comparison to the respective normal ranges of the human foot [16], which show that the HURL possesses the structural capability of replicating the human-like ankle movements displayed in Fig. 2, while covering, and in most cases exceeding, the normal range of the human ankle.

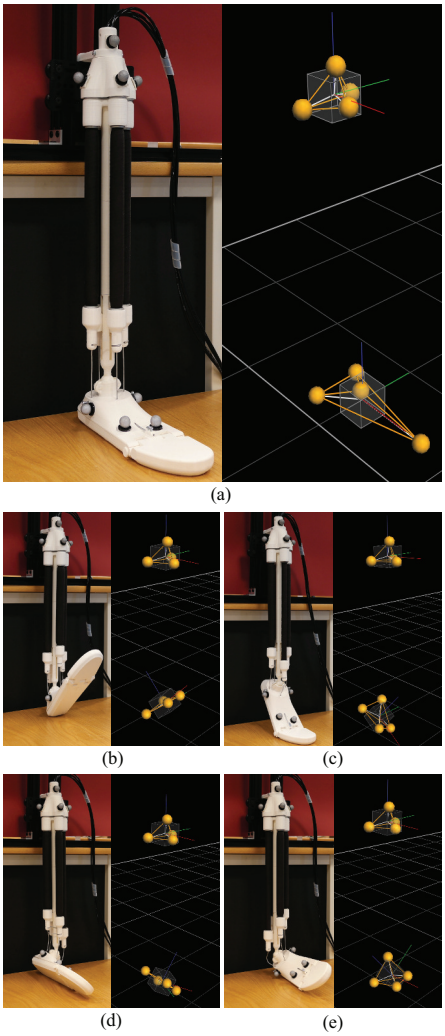

Fig. 4. Photographic stills and images acquired via the VICON motion capturing system of the HURL prototype during: (a) Idle, (b) Dorsiflexion, (c) Plantar Flexion, (d) Eversion, and (e) Inversion.

TABLE I. RANGE OF MOTION OF THE HURL PROTOTYPE

i	Ankle Movement	Maximum Angle [°]	
		HURL	Human Foot
1	Dorsiflexion	41.2	~ 20
	Plantar Flexion	39.5	~ 40
2	Eversion	39.0	~ 25
	Inversion	39.3	~ 35

Following the open-loop experimental evaluation, the proposed ANPID-based structure undertakes the angular control of multiple dorsiflexion/plantar flexion an eversion/inversion experimental sequences, with the constraints posed on the respective process values θ_1 and θ_2 specified as $[\theta_{1,\min}, \theta_{1,\max}] = [-39.4, 41.3]^o$ and $[\theta_{2,\min}, \theta_{2,\max}] = [-39.3, 39.1]^o$. For these experiments, the ANPID mode selectors were empirically adjusted at $f = 0.75$ and $q = 0$, leading to a linearly adjustable proportional action for balanced disturbance rejection and set-point tracking, along with a measurement-affected derivative action for reduced derivative kick effect in cases of sudden set-point alterations. The linearity factor g was set to $g = 0.81$, in order to achieve a smooth non-linear adjustment of the error signal and a decrease of the K_p gain at low error magnitudes. Finally, the gain scheduler's control parameters $K_{P,m}$, $T_{I,m}$ and $T_{D,m}$ are tuned via fine-tuning through extensive experimental trials and their values, with respect to the PMA's operating regions.

Multiple set-point experiments were performed to test the efficacy of the ANPID-based control scheme regarding the HURL's movements. In these trials every DoF is tested separately, while the other one is kept at idle state. The experimentally acquired responses are presented in Figs. 5 and 6, respectively, where the multiple reference signals are indicated with red dotted lines and the experimental angular θ_1 and θ_2 responses are displayed with blue solid lines. The obtained experimental responses reveal smooth and fast convergence for all test-cases with absence of major transient phenomena. With rising times remaining under half of a second and the mean absolute steady-state errors ranging between 0.02^o – 0.10^o for the dorsiflexion/plantar flexion and 0.03^o – 0.11^o for the eversion/inversion movements, these set-point experiments indicate the setup's capability to accurately replicate the motion capabilities of the human ankle via the utilization of the proposed control structure.

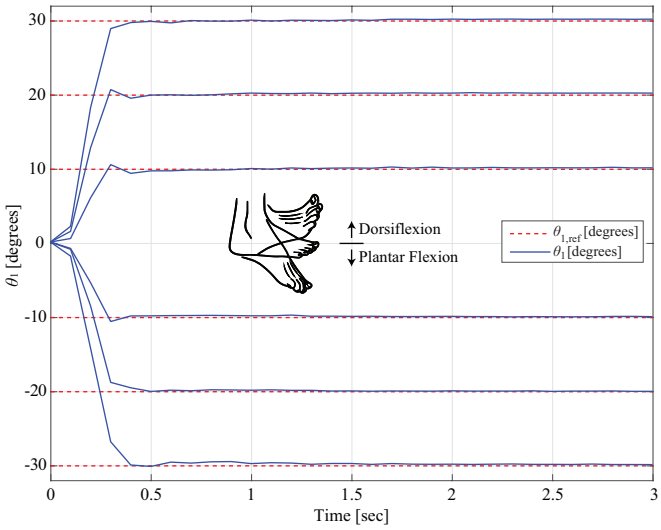

Fig. 5. Set-point experiments for the evaluation of the HURL's dorsiflexion and plantar flexion movement capabilities.

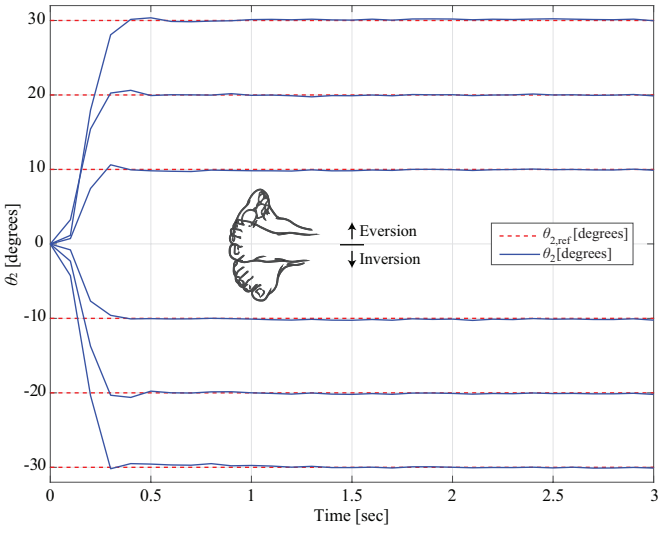

Fig. 6. Set-point experiments for the evaluation of the HURL's eversion and inversion movement capabilities.

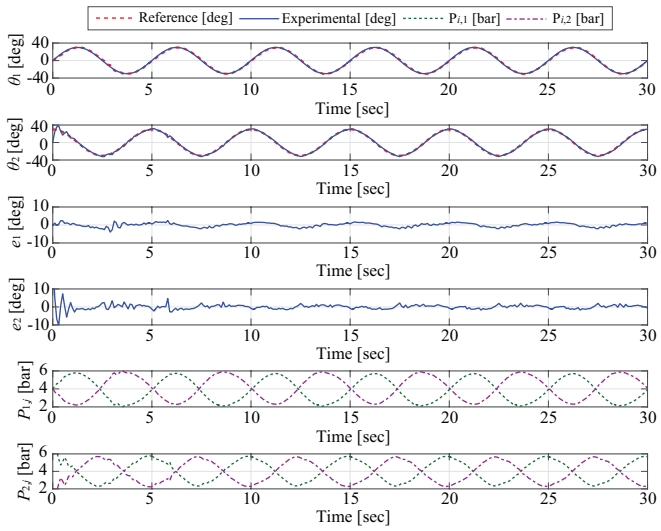

Fig. 7. Closed-loop responses during tracking of sinusoidal reference signals for both dorsiflexion/plantar flexion and eversion/inversion patterns.

In the sequel, experimental studies were performed with the HURL freely suspended for the preliminary evaluation of the system's ability to track both movement patterns at the same time. Specifically, angular responses of θ_1 and θ_2 for a sinusoidal reference signal ranging between -30° – 30° at 0.2 Hz, while being characterized by a 90° phase difference, are depicted in Fig. 7, along with their respective error signals $e_i=\theta_{i,\text{ref}}-\theta_i$ and pressure control efforts $P_{\text{i,j}}$. The performance quality of the control structure is maintained, providing smooth tracking in both cases despite the selected angular reference input covers a large part of the HURL's operational range, as well as the frequency of the reference signals by taking into account the inherently large settling times of the utilized PMAs. The mean absolute error of the proposed scheme remains at low values and is measured at 0.89° for the dorsiflexion/plantar flexion and 0.84° for the eversion/inversion movements. It has to be noted that the same control performance is also maintained for higher frequencies, with the evaluation of the HURL performance in such challenging scenarios being a part of ongoing work.

The experimental results presented in this Section prove the conceptual assumption of a design where its 2 DoFs are mechanically decoupled and can be successfully controlled via two independent controllers, thus highlighting the design's advantage of simplifying the complexity of this demanding motion control problem. In overall, the experimental evaluation reveals that this novel endoskeletal design approach possesses the structural attributes necessary for biomimetic reproduction of the basic movements of the human ankle and enables the expansion of this design the proposed 10-DoF lower-limb configuration.

VI. Conclusions

In this article, the design and development problem of a HUmanoid Robotic Leg (HURL) prototype was addressed, which was designed to provide an alternative to existing robotic ankle-mimicking devices. For the evaluation of the conceptual design strategy, a feasibility study was performed via the development of a 2-DoF prototype and the results of a preliminary experimental evaluation of its motion capabilities (extension-flexion, ulnar-radial deviation) were presented. Multiple tracking sequences were performed via an advanced non-linear PID-based control algorithm and the acquired results proved that the HURL possesses the structural attributes necessary for biomimetic reproduction of the basic movements of the human ankle.

References

[1] R. Drake, Gray's Anatomy for Students, Third Edition, Elsevier, 2015.

[2] G. Andrikopoulos, G. Nikolakopoulos, and S. Manesis, "A Survey on applications of Pneumatic Artificial Muscles," in *Mediterranean Conference on Control and Automation* (MED), 2011, pp. 1439-1446.

[3] G. Andrikopoulos, G. Nikolakopoulos, and S. Manesis, "Pneumatic Artificial Muscles: A Switching Model Predictive Control Approach", in *Control Engineering Practice* (CEP), Elsevier, vol. 21, no. 12, pp. 1653-1664, December 2013.

[4] R. Versluys, J. Naudet, B. Vanderborght, G. Lenaerts, and D. Lefeber, "IPPMA: Intelligent Prosthesis actuated by pleated Pneumatic Artificial Muscles: Objectives and Mechanical Concept," in *International Conference on Climbing and Walking Robots* (CLAWAR), 2006, pp. 1–9.

[5] K. A. Tahboub, "Biologically-inspired humanoid postural control," J. Physiol. Paris, vol. 103, no. 3–5, pp. 195–210, 2009.

[6] R. W. Colbrunn, G. M. Nelson, and R. D. Quinn, "Design and Control of a Robotic Leg with Braided Pneumatic Actuators," in *IEEE/RSJ International Conference on Intelligent Robots and Systems*, 2001, vol. 2, pp. 992–998.

[7] B. Vanderborght, B. Verrelst, R. Van Ham, J. Naudet, J. Vermeulen, D. Lefeber, and F. Daerden, "LUCY, a Bipedal Walking Robot with Pneumatic Artificial Muscles," *Mechatronics*, 2004.

[8] R. Niiyama, S. Nishikawa, and Y. Kuniyoshi, "Athlete robot with applied human muscle activation patterns for bipedal running," in *10th IEEE-RAS International Conference on Humanoid Robots*, 2010, pp. 498–503.

[9] J. Lei, J. Wu, and H. Yu, "Analysis on the musculoskeletal leg mechanism driven by PMAs," in *IEEE International Conference on Mechatronics and Automation*, 2014, pp. 1659–1663.

[10] T. Takuma, S. Hayashi, and K. Hosoda, "3D bipedal robot with tunable leg compliance mechanism for multi-modal locomotion," *IEEE/RSJ Int. Conf. Intell. Robot. Syst.*, pp. 1097–1102, Sep. 2008.

[11] K. Narioka, S. Tsugawa, and K. Hosoda, "3D limit cycle walking of musculoskeletal humanoid robot with flat feet," *IEEE/RSJ Int. Conf. Intell. Robot. Syst.*, pp. 4676–4681, Oct. 2009.

[12] F. H. Netter. Atlas of Human Anatomy. Sixth Edition. W. B. Saunders Company. 2014.

[13] G. Andrikopoulos, G. Nikolakopoulos, and S. Manesis, "Advanced Non-linear PID Based Antagonistic Control for Pneumatic Muscle Actuators", in *IEEE Transactions on Industrial Electronics* (TIE), vol. 61, no. 12, pp. 6926–6937, December 2014.

[14] K. J. Åström, and T. Hagglund, "PID Controllers: Theory, Design and Tuning", *Instrument Society of America*, pp. 343, 1995.

[15] D. Winter, Biomechanics and Motor Control of Human Movement. Fourth Edition. John Wiley & Sons, Inc. 2009.

[16] B. M. Nigg, V. Fisher, T. L. Allinger, J. R. Ronsky, and J. R. Engsberg, "Range of motion of the foot as a function of age," *Foot Ankle,* vol. 13, no.6, pp. 336-343, Jul-Aug 1992.